

CCD photometry of galactic open star clusters—IV. NGC 366

A. K. Pandey, B. C. Bhatt, V. Mohan, D. C. Paliwal and H. S. Mahra

Uttar Pradesh State Observatory, Manora Peak, Naini Tal 263 129

Received 1993 August 27; accepted 1993 November 12

Abstract. CCD photometry of the open cluster NGC 366 has been carried out in *UBVRI* photometric passbands down to 19.5 mag. It is found that the reddening is non-uniform across the cluster field, having $\Delta E(B - V) = 0.30$ mag. A distance of 2.15 kpc and an age of 25 Myr have been obtained for the cluster. A comparison of the luminosity function (LF) of the cluster with the LFs of other young clusters, shows that the cluster LFs agree fairly well towards the higher mass end, whereas there is substantial variation in the LFs of the clusters towards fainter end. It is concluded that there is a significant excess of low mass stars in NGC 366 as compared to NGC 1931 and other young clusters.

Key words : open cluster—photometry

1. Introduction

Open star clusters can be used to trace the evolution of the Galaxy and its present dynamical state. Open clusters are also good tools to analyse the large scale properties of the disk of the Galaxy and to test the theories of stellar and galactic evolution (cf. Janes 1979; Janes & Adler 1982; Pandey *et al.* 1988; Palous *et al.* 1977). To obtain fundamental information for such studies cluster's distance, age and interstellar extinction inside the star clusters are mandatory which can be derived from the colour-magnitude and the colour-colour diagrams of star clusters. Such observations are lacking for most of the distant open star clusters. With the introduction of charge coupled devices (CCD), it is now possible to have observations of previously unstudied open clusters with a moderate sized (~ 1 -metre class) telescope to study the evolutionary aspects of these unobserved open clusters as well as to increase the data base for testing the available models of stellar and galactic evolution.

In this paper we describe the *UBVRI* CCD photometric observations of the stars in the field of NGC 366. The open cluster NGC 366 (C0103 + 619), ($l = 124^\circ.68$, $b = -0^\circ.59$) has been classified as Trumpler class II 3 m (Lynga 1987). These observations have been used to study interstellar extinction across the cluster region and to estimate age, distance and luminosity function of the cluster.

2. Observations

The observations of NGC 366 were carried out in *U*, *B*, *V*, *R* and *I* passbands using the Photometrics CCD system having a 384×576 pixels Thomson chip, at $f/13$ Cassegrain focus of the 104-cm reflector of the Uttar Pradesh State Observatory (UPSO) during October 1992 and January 1993. In this set up, the entire CCD chip covers a field of 2.0×3.0 sq arc-min of the sky. In order to improve the *S/N* ratio, the observations were taken at 2×2 binning mode. The details of the present CCD system have also been described by Bhatt (1993) and Mohan *et al.* (1991). The cluster region was observed in two overlapping fields, which have been named as North and South fields of the cluster (figures 1a and 1b), in each passbands. The multiple exposures were taken with exposure time ranging from 8 to 1800 seconds

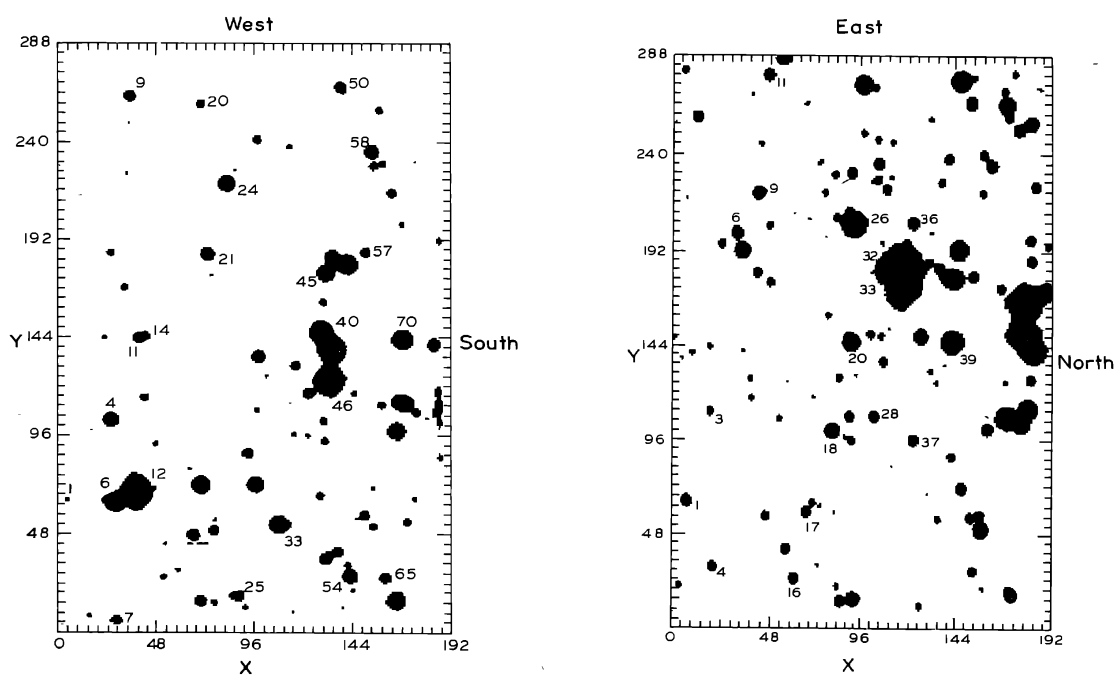


Figure 1a. Identification map for the North region of the cluster NGC 366.

Figure 1b. Identification map for the South region of the cluster NGC 366.

depending upon the presence of bright stars and filter used and the frames were coadded in order to achieve a total integration time of 60 minutes in *U*, 30 minutes in *B* and *V* and 5 minutes in *R* and *I* filters. The observing details are given in table 1. A number of flats were taken in each passband by observing the twilight sky. Landolt (1983) standard stars were also observed for calibration purposes.

3. Data reduction

The observations have been reduced using the Micro Vax II system of UPSO. Clean images have been obtained using the ESO MIDAS software package. The cleaned frames in each filter having similar exposure times were coadded. The photometry was carried out using the DAOPHOT profile-fitting software (Stetson 1987). The stellar point-spread-function (PSF) was evaluated from several uncontaminated stars present in each frame. For a few bright

Table 1. Details of observations

Filter	North region				South region			
	23/24 Oct 92		2/3 Oct. 92		22/23 Oct. 92		12/13 Jan. 93	
	a	b	a	b	a	b	a	b
<i>U</i>	2	1800			2	1800	2	300
<i>B</i>	3	600			2	900	2	120
	2	100			1	150		
<i>V</i>	2	300			3	600	1	30
	1	60					1	40
<i>R</i>	2	150	1	300			2	10
	1	10	1	180				
			1	8				
<i>I</i>	2	150	1	300			2	10
	1	10	1	180				
			1	10				

Note Columns a and b for each night show the number of frames observed and exposure time in seconds respectively

stars which were saturated in long exposure frames, short exposure frames were used. The *X* and *Y* coordinates as well as photometric data of the stars measured in the North and South cluster fields are given in table 2. The cluster was observed on different nights and the night to night variations in the observations have been estimated using the common stars brighter than 17.0 mag in the overlapping area. The photometric errors of observations ($\pm\sigma$) are found to be 0.018, 0.023, 0.032, 0.017 and 0.024 mag in *V*, (*B* – *V*), (*U* – *B*), (*R* – *I*) and (*V* – *I*) respectively.

4. Interstellar extinction

To estimate the interstellar extinction in the cluster region, we have used the (*U* – *B*, *B* – *V*) diagram shown in figure 2. The intrinsic zero-age-main-sequence (ZAMS) given by Schmidt-Kaler (1982) was fitted to the main-sequence stars of spectral type earlier than A0 in the cluster field. The minimum and maximum reddening values estimated by sliding fit method come out to be $E(B - V)_{\min} = 1.10$ mag and $E(B - V)_{\max} = 1.40$ mag. The slope $E(U - B)/E(B - V)$ was taken to be equal to 0.72 (Johnson & Morgan 1953). The observed dispersion of 0.3 mag in the $E(B - V)$ values cannot be explained due to errors in the data and other parameters such as rotation, duplicity etc. which can produce a maximum variation of 0.11 mag in $E(B - V)$ for MS stars (cf. Burki 1975). Therefore, we conclude that the reddening is non-uniform across the cluster field. The interstellar extinction for individual MS stars has also been derived using the Q-method (Johnson & Morgan 1953) and these values have been used in subsequent analysis.

5. Distance to the cluster

The colour-magnitude diagrams (*V*, *B* – *V*), (*V*, *U* – *B*) and (*V*, *V* – *I*) are plotted in figures 3, 4 and 5 respectively. A broad but well defined cluster MS is clearly visible down to 19.5

Table 2. Magnitudes and colours of the stars in the field of NGC 366

Star ID	X	Y	(U - B)	(B - V)	V	(R - I)	(V - I)	Remark
<i>North region</i>								
1	3.78	64.70	*	1.507	18.736	1.068	1.983	m
2	14.43	5.49	*	2.267	18.336	1.066	1.662	
3	22.50	147.55	*	1.438	18.720	1.084	1.991	m
4	25.35	105.27	0.410	1.134	14.897	0.769	1.370	M
5	25.68	190.74	*	1.494	17.937	1.037	1.817	m
6	27.08	63.26	1.096	1.146	13.832	0.609	1.192	
7	28.00	1.79	*	2.596	17.510	1.540	3.134	
8	33.92	231.33	*	1.752	18.890	1.105	2.058	m
9	35.42	270.81	0.652	1.109	16.103	0.748	1.329	M
10	37.60	18.47	*	1.318	19.330	1.059	2.019	
11	39.55	147.39	0.685	1.231	16.522	0.848	1.525	M
12	39.63	69.73	0.218	1.224	11.531	0.832	1.430	M
13	42.30	116.73	*	1.321	17.235	0.841	1.491	m
14	42.92	148.29	*	1.334	17.179	0.923	1.544	m
15	48.07	92.88	*	1.649	18.343	0.974	1.784	m
16	51.73	25.13	*	1.311	18.030	0.904	1.670	m
17	66.89	46.63	0.498	1.118	15.738	0.759	1.334	M
18	70.38	12.73	0.592	1.083	16.114	0.757	1.304	M
19	70.54	72.12	0.206	1.080	14.125	0.764	1.325	M
20	71.31	266.52	*	1.680	17.812	1.068	2.033	
21	74.58	190.16	0.492	1.149	15.487	0.819	1.485	M
22	77.25	48.87	0.919	1.216	16.687	0.838	1.472	M
23	77.46	11.95	*	1.469	18.040	0.968	1.696	m
24	84.16	226.07	0.475	1.100	14.644	0.791	1.448	M
25	90.08	15.52	0.889	1.321	16.690	0.829	1.530	M
26	92.89	9.64	*	1.677	18.426	1.036	1.778	m
27	94.86	88.03	*	1.584	17.359	1.112	2.076	
28	98.32	72.36	0.496	1.197	14.834	0.843	1.481	M
29	99.32	110.39	*	1.526	18.295	1.047	1.854	m
30	99.76	248.15	*	1.433	17.531	0.959	1.826	m
31	99.95	137.70	0.527	1.164	15.736	0.835	1.487	M
32	104.27	127.90	*	1.387	18.817	0.981	1.939	
33	109.71	52.21	0.378	1.156	14.130	0.798	1.413	M
34	116.12	244.62	*	1.197	18.089	0.837	1.576	
35	117.75	97.69	*	1.445	18.457	1.079	1.934	m
36	118.64	133.08	0.780	1.113	16.745	0.798	1.391	M
37	124.86	97.16	*	1.722	18.812	1.129	2.027	m
38	125.06	118.68	0.704	1.246	16.735	0.835	1.561	M
39	130.97	66.75	*	1.354	17.462	0.850	1.585	m

(Continued)

Table 2. Continued

Star ID	<i>X</i>	<i>Y</i>	(<i>U</i> – <i>B</i>)	(<i>B</i> – <i>V</i>)	<i>V</i>	(<i>R</i> – <i>I</i>)	(<i>V</i> – <i>I</i>)	Remark
40	131.32	150.40	0.165	0.971	13.109	0.778	1.281	M
41	132.74	165.27	*	1.533	17.892	1.049	1.830	m
42	132.84	104.60	*	1.387	17.784	0.978	1.748	m
43	133.42	94.10	0.875	1.443	17.734	0.943	1.687	M
44	133.78	34.91	0.883	1.243	16.009	0.821	1.447	M
45	133.83	180.25	0.452	1.155	14.700	0.868	1.601	M
46	135.31	125.39	0.157	1.056	11.929	0.786	1.283	M
47	136.69	141.80	0.154	0.965	12.282	0.833	1.207	M
48	137.14	188.55	0.753	1.241	15.579	0.954	1.767	
49	139.58	37.94	0.797	1.093	16.418	0.772	1.348	M
50	141.64	275.28	0.875	1.073	16.357	0.767	1.435	M
51	141.99	9.28	*	1.759	18.602	1.015	1.741	M
52	144.59	184.77	0.223	0.953	13.701	0.758	1.363	M
53	145.72	25.61	0.329	0.910	14.728	0.647	1.125	M
54	147.12	18.25	*	1.507	18.432	0.844	1.609	M
55	148.11	118.81	*	1.304	18.304	0.985	1.783	
56	153.09	56.65	0.798	1.176	16.561	0.795	1.391	M
57	154.26	190.87	1.078	1.036	16.932	0.821	1.637	M
58	157.17	242.23	1.052	1.298	15.690	0.902	1.729	
59	157.43	51.00	*	1.480	17.765	0.913	1.639	m
60	157.63	70.40	*	1.792	18.728	1.034	1.900	m
61	158.07	235.01	*	1.455	17.788	0.923	1.810	m
62	161.16	263.36	*	1.157	17.753	0.854	1.651	m
63	161.85	112.92	*	1.583	17.907	0.993	1.832	m
64	162.85	235.90	*	1.566	18.290	0.990	2.013	m
65	163.48	24.59	*	2.237	17.381	1.313	2.423	
66	167.19	221.28	0.943	1.037	16.991	0.794	1.493	
67	168.74	13.23	0.142	0.870	13.772	0.612	1.060	M
68	169.18	99.40	0.403	1.221	14.439	0.838	1.502	M
69	171.02	114.59	0.610	1.392	14.874	0.782	1.687	M
70	172.16	146.53	0.286	1.368	13.837	0.880	1.613	M
71	172.37	205.23	*	1.248	18.265	0.949	1.838	
<i>South region</i>								
1	7.54	57.88	*	1.114	16.904	0.822	1.575	m
2	12.01	253.71	*	1.663	17.673	1.041	1.984	
3	19.08	103.60	*	1.402	18.485	1.012	1.975	m
4	20.79	24.31	*	1.743	18.333	1.089	2.222	
5	24.54	189.11	*	1.578	18.430	0.943	1.868	m
6	32.25	194.85	0.922	1.255	16.689	0.829	1.539	m

(Continued)

Table 2. Continued

Star ID	X	Y	$(U - B)$	$(B - V)$	V	$(R - I)$	$(V - I)$	Remark
7	34.78	185.70	0.278	1.028	15 094	0.725	1 314	M
8	42.59	174.34	*	1 438	17.947	0 981	1.821	m
9	42.72	215.15	*	1.354	16.778	0 898	1 648	m
10	47.31	50.40	*	1 332	18.074	0.939	1.833	m
11	47.74	275.41	0.727	1 206	16.657	0 771	1.394	M
12	48.56	198.60	*	1.609	18 759	1.046	1 975	M
13	49.11	169.44	*	1 613	18.176	0.994	1.806	m
14	54.89	284.28	0.246	1.076	14.925	*	0.939	M
15	57.52	33.79	*	1.092	17.274	0 748	1 463	m
16	61.73	18.69	0.848	1.088	17.033	0.777	1.453	
17	67.85	52.47	*	1.103	17 380	0 782	1 482	m
18	80.70	94.03	0.593	1.186	15 727	0 816	1 554	M
19	81.53	224.83	*	1 509	18.828	0.996	1.964	m
20	84.08	121.15	*	1.551	18 759	1.057	2.070	m
21	89.32	101.50	*	1 255	17.253	0.875	1 567	m
22	90.01	225.73	*	1 239	17 045	0.798	1.456	m
23	90.02	139.25	0.361	1.174	14 924	0.846	1.519	M
24	90.59	89.03	*	1.485	18.600	0.974	1 974	m
25	91.06	199.76	1 720	2.022	14.233	1.245	2.371	
26	95.49	270.83	0.392	0.961	14.202	0.572	1 075	M
27	99.93	143.52	*	1 458	18.685	1.011	1.984	m
28	101.80	101.58	*	1.332	17.217	0 913	1 691	m
29	103.62	230.51	0.795	1.215	16 812	0.796	1.415	M
30	106.23	129.54	*	1.502	18.007	0.944	1 753	m
31	107.64	217.30	*	1.270	17 525	0.855	1.542	m
32	114.00	180.00	0.194	1 134	11.482	0.810	1.480	M
33	114.77	163.33	0.364	1 232	13 504	0.917	1.642	M
34	118.00	178.00	0.267	1.177	12 239	0.801	1.441	M
35	118.11	182.69	0 270	1 468	14 000	*	1.122	M
36	121.10	200.40	0.862	1.176	16 614	0 792	1.415	M
37	121.64	89.50	*	1 335	17 258	0 885	1.634	m
38	125.17	142.44	0 793	1.340	16 099	0.929	1.659	
39	130.25	125.14	*	0.908	19.387	1.047	1 988	
40	134.32	49.58	*	1 574	18.925	1.008	1 930	m
41	135.62	221.28	*	1 587	18 512	1.043	1.958	m

Notes *Observations not available; m and M—cluster members (see text)

mag. To estimate the distance to the cluster we have fitted the ZAMS given by Schmidt-Kaler (1982) in the $(V, B - V)$ and $(V, U - B)$ colour-magnitude diagrams (CMDs) and the ZAMS given by Walker (1985) in the $(V, V - I)$ CMD on the bluest envelope of data points in figures 3, 4 and 5 and a distance modulus of 15.7, 15.4, and 15.5 mag have been obtained from these three CMDs respectively. We have adopted the relation $E(V - I) = 1.25 \times E(B - V)$ (Walker 1985) to estimate distance modulus from figure 5 and it seems that the slope

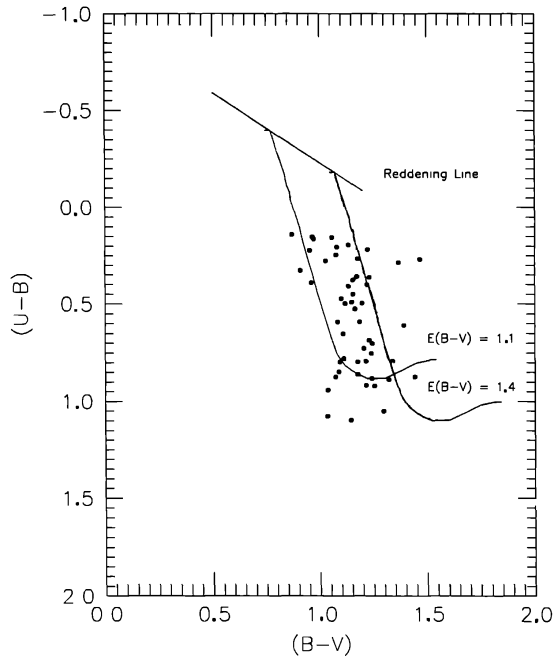


Figure 2. The colour-colour diagram for the stars in the cluster region.

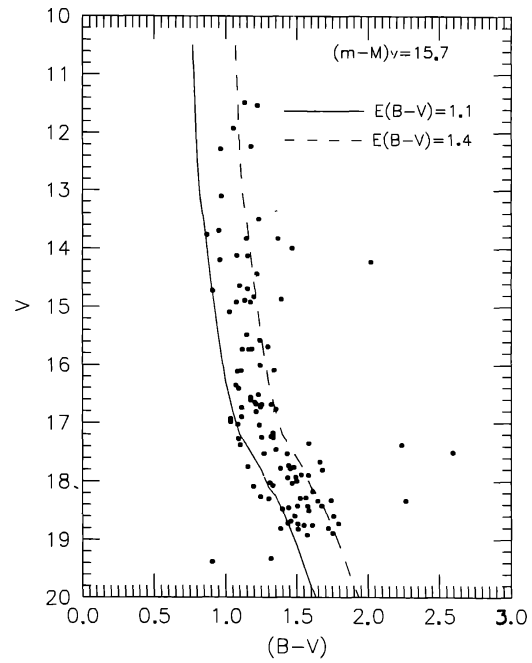


Figure 3. The colour-magnitude diagram ($V, B - V$) for all stars measured in the North and South regions of NGC 366. The full line and dashed line represent the ZAMS given by Schmidt-Kaler (1982) for minimum and maximum reddening values respectively.

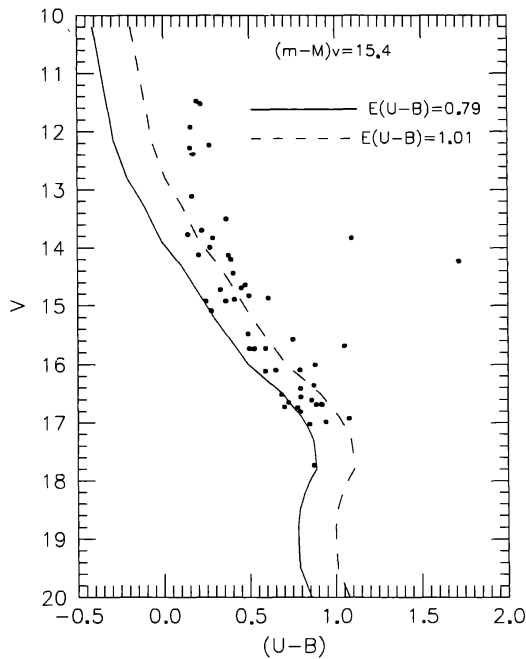


Figure 4. The colour-magnitude diagram ($V, U - B$) for all stars measured in the North and South regions of NGC 366. The full line and dashed line represent the ZAMS given by Schmidt-Kaler (1982) for minimum and maximum reddening values respectively.

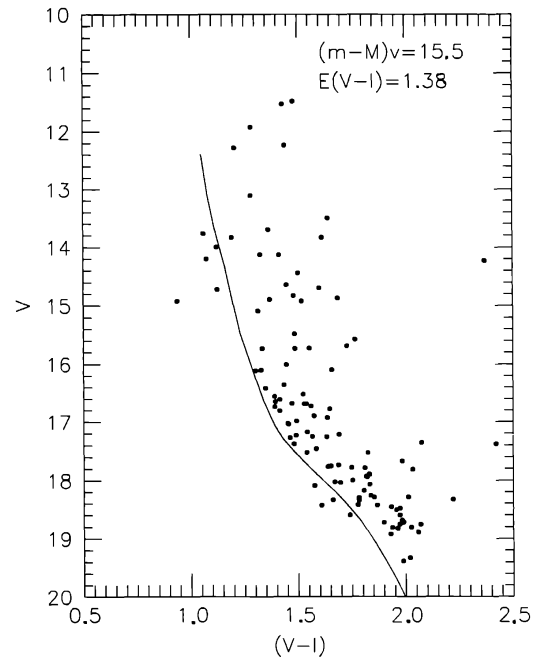


Figure 5. The colour-magnitude diagram ($V, V - I$) for all stars measured in the North and South regions of NGC 366. The full line represents the ZAMS given by Walker (1985).

of 1.25 is valid for this cluster, however, different slopes have been obtained for other clusters, e.g. Bhatt *et al.* (1993b) have found a slope of 1.36 for the open cluster NGC 7419 and Alcalá & Ferro (1988) have obtained a value of 1.68 for NGC 7790.

Using the mean $E(B - V) = 1.25$ mag for the cluster and the most acceptable value of $R = 3.1$, the $A_v = 3.1 \times 1.25$, mean true distance modulus $(m - M)_0$ comes out to be 11.66 ± 0.15 (s.e.) mag which corresponds to a distance of 2.15 ± 0.13 (s.e.) kpc.

6. Membership

Since the proper motion and spectroscopic studies are not available for the stars in the cluster region, the discrimination of non-members from the observed sample has been carried out using the photometric and statistical criteria. We have considered only those stars as members which lie in between the blue and the red envelopes of the MS obtained by shifting the MS for the maximum value of $E(B - V)$ in the $(V, B - V)$ CMD. The stars found inside this belt have been considered as cluster members and these are denoted as 'm' in table 2. The unreddened colour-magnitude diagrams, $[V_0, (B - V)_0]$ and $[V_0, (U - B)_0]$ are plotted in figures 6 and 7 respectively. The main-sequence shifted by 0.75 mag in V_0 is also shown by dashed line in both the CMDs to account for the possible widening of the MS due to binary stars etc. The stars found in this belt are considered as cluster members with a greater probability and these stars are assigned as 'M' in table 2.

7. Age of the cluster

To estimate the age of the cluster we have used the observations of those stars for which individual reddening could be obtained. The $[M_v, (B - V)_0]$ and $[M_v, (U - B)_0]$ diagrams for cluster member stars are shown in figures 8 and 9 respectively. The age of the post-main-

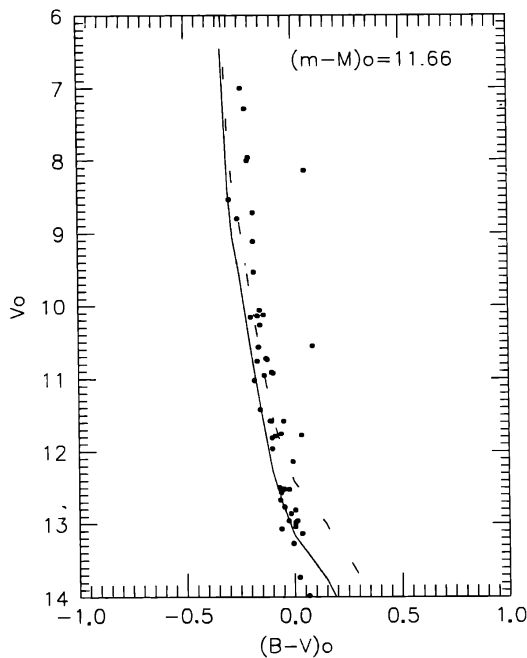


Figure 6. The $[V_0, (B - V)_0]$ diagram of NGC 366.

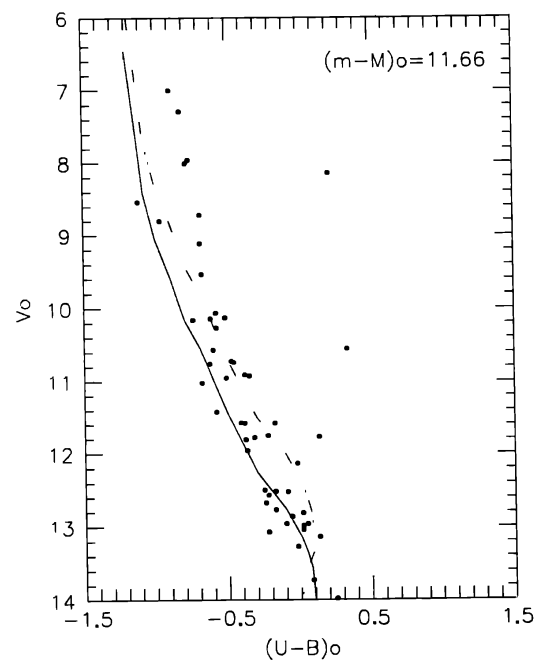


Figure 7. The $[V_0, (U - B)_0]$ diagram of NGC 366.

sequence stars has been estimated using the empirical isochrones given by Mermilliod (1981). From the $[M_v, (U - B)_0]$ and $[M_v, (B - V)_0]$ diagrams it is inferred that the age of the cluster lies between the ages of NGC 457 (age $\sim 10^7$ yr) and IC 4665 (age $\sim 3.63 \times 10^7$ yr) groups. In figures 10 and 11 we have fitted the theoretical isochrones given by Maeder & Maynet (1991) for the $\log \text{age} = 7.4$. Thus, we infer that the age of the cluster NGC 366 is about 25 Myr.

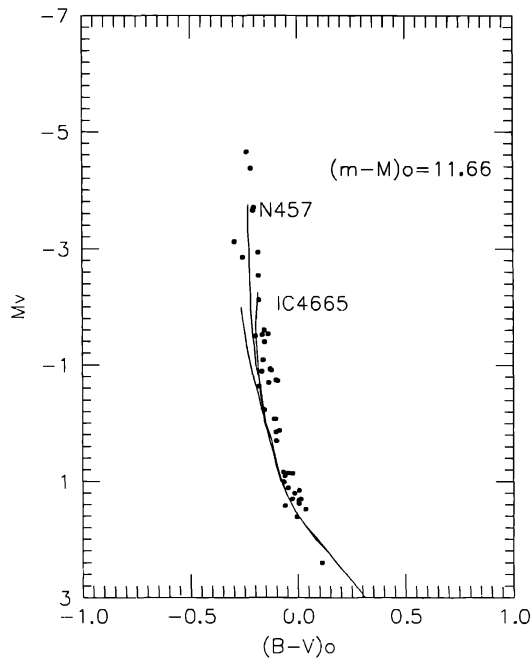


Figure 8. The $[M_v, (B - V)_0]$ diagram of the member stars in NGC 366. The solid curves are isochrones given by Mermilliod (1981).

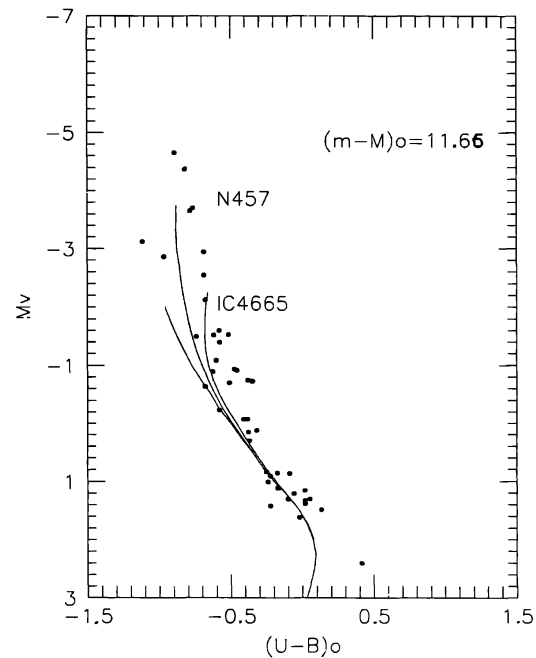


Figure 9. The $[M_v, (U - B)_0]$ diagram of the member stars in NGC 366. The solid curves are isochrones given by Mermilliod (1981).

8. Luminosity function

We have also observed two field regions located at ~ 30 arc-minutes towards West and North directions from the cluster region to estimate the luminosity function (LF) as described by Bhatt *et al.* (1993b). The LF for the cluster is shown in figure 12 and this has been compared with the LF of the NGC 581, NGC 663 and NGC 1931. The data of NGC 581, NGC 663 have been taken from Phelps and Janes (1991a, b) and for NGC 1931, data have been taken from Bhatt *et al.* (1993a). The number of stars were normalised at $M_v = 1.0$ mag. Towards the higher mass end the LF, within uncertainty levels, is nearly alike to the LFs of the other young clusters, but towards the low mass end it is quite different from the LFs of the other young clusters. It is concluded that cluster has a large number of low mass stars as compared to other young clusters. The LF for the cluster has also been compared with that of field stars given by Scalo (1986). The data have been normalised for the magnitude bin 17.0-18.0 mag, considering that $V = 18.0$ mag represents a limit where our photometry is reasonably complete. It seems that LF for the cluster is different from that of field stars given by Scalo (1986). The LF obtained for the cluster stars which lie in between the blue and red envelope of the MS in the $(V, B - V)$ CMD also agrees fairly well with the

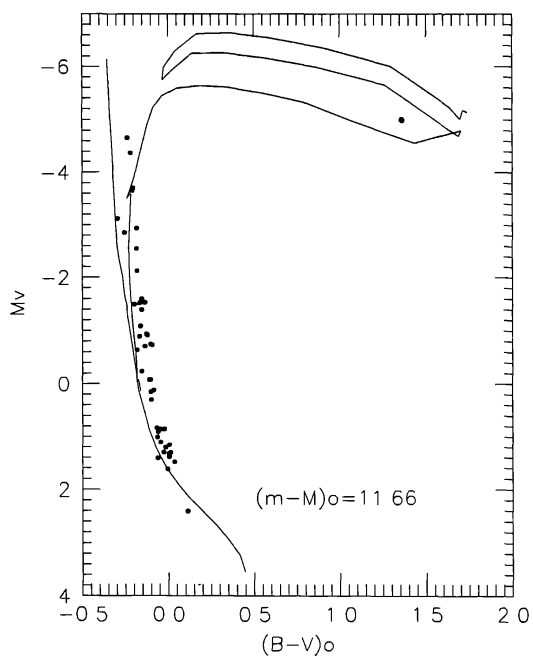


Figure 10. The $[M_v, (B - V)_0]$ diagram of the member stars in NGC 366. The solid curves are isochrones given by Maeder & Maynet (1991).

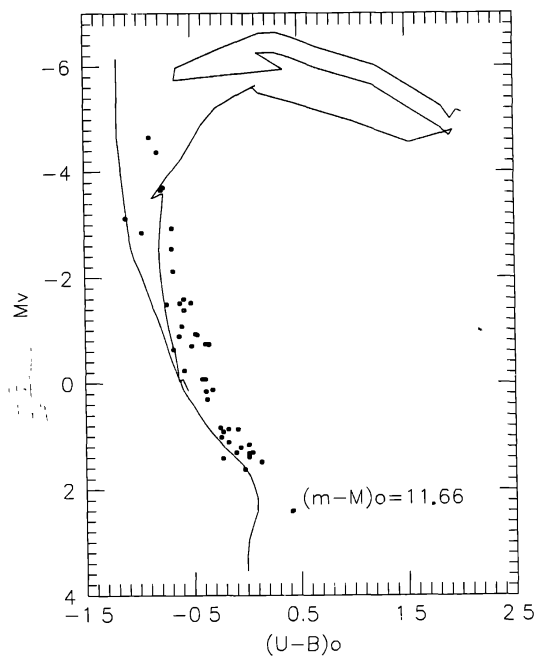


Figure 11. The $[M_v, (U - B)_0]$ diagram of the member stars in NGC 366. The solid curves are isochrones given by Maeder & Maynet (1991).

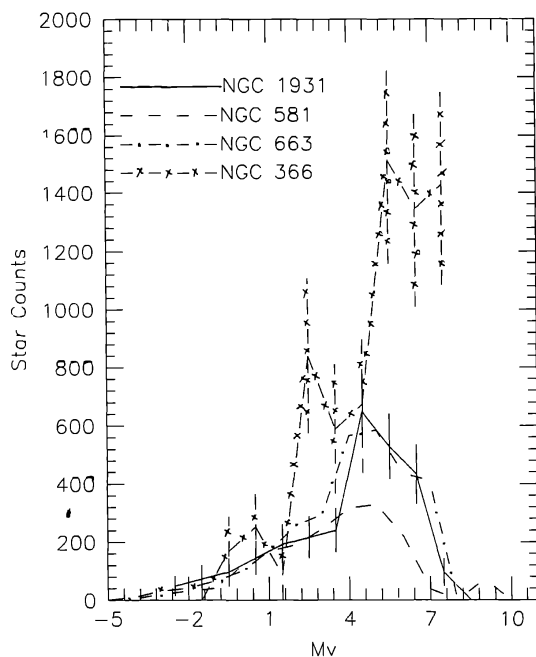


Figure 12. The luminosity function of the cluster stars in NGC 366. The error bars corresponding to \sqrt{N} are also shown in the figure.

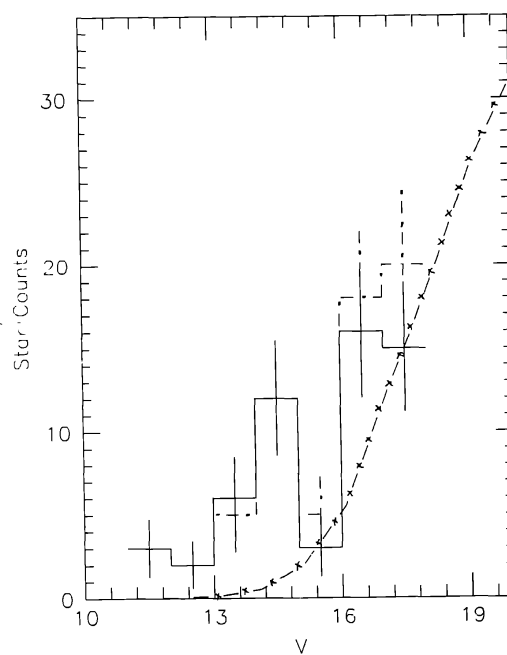


Figure 13. The luminosity distribution of the stars in NGC 366. The error bars corresponding to \sqrt{N} are also shown in the figure. — Cluster stars from statistical criteria; —•— Cluster stars inside the belt of CMD; —x—x— LF of field stars (Scalo 1986).

LF obtained by statistical method and a comparison is shown in figure 13. Thus it seems that the stars which lie between the two envelopes can be taken as possible members with less uncertainty.

9. Conclusions

The CCD photometry of the cluster NGC 366 in *UBVRI* photometric passbands down to 19.5 mag manifests a true distance modulus of 11.66 mag corresponding to a distance of 2.15 kpc. The age of the cluster is estimated to be ~25 Myr. The reddening in the cluster region is found to be variable having $\Delta E(B - V) = 0.30$ mag. The LF of NGC 366 has been compared with the LF of the other young open clusters and it is found that there are considerably larger number of low mass stars in the cluster as compared to other young clusters.

References

- Alcala J. M., Ferro A. A., 1988, *Rev. Mex. Astron. Astrof.*, 16, 81
 Bhatt B. C., 1993, Ph.D. Thesis, Kumaon Univ., Naini Tal.
 Bhatt B. C., Pandey A. K., Mahra H. S., Paliwal D. C., 1993a, BASI, (submitted)
 Bhatt B. C., Pandey A. K., Mohan V., Mahra H. S., Paliwal D. C., 1993b, BASI, 21, 33
 Burki G., 1975, *A&A*, 43, 37.
 Janes K., Alder D., 1982, *ApJS*, 49, 425.
 Janes K. A., 1979, *ApJS*, 39, 135.
 Johnson H. L., Morgan W. W., 1953, *ApJ*, 117, 313.
 Landolt A. U., 1983, *AJ*, 88, 439.
 Lynga G., 1987, *Catalogue of Open Clusters 1/I C7030*, Centre de Données Stellaires, Strasbourg.
 Maeder A., Maynet G., 1991, *A&A*, 89, 451.
 Mermilliod J. C., 1981, *A&A*, 97, 235.
 Mohan V., Paliwal D. C., Mahra H. S., 1991, BASI, 19, 235.
 Palous J., Ruprecht J., Dluhnevskaya O. B., Piskunov T., 1977, *A&A*, 61, 27.
 Pandey A. K., Bhatt B. C., Mahra H. S., 1988, *A&A*, 189, 66.
 Phelps R. L., Janes K. A., 1991a, in *Precision Photometry: Astrophysics of the Galaxy*, ed. A. G. Davis Philip, L. Davis Press, Schenectady, p. 331
 Phelps R. L., Janes K. A., 1991b, *Mem. Soc. Astr. Ital.*, 62, 507
 Scalzo J. M., 1986, *Funda. Cosmic Phys.*, 11, 1
 Schmidt-Kaler Th., 1982, *Landolt-Bornstein, Numerical Data and Funct. Relationship in Sci. and Tech. New Ser.*, Group 6, Vol. 2b, p. 1
 Stetson P. B., 1987, *PASP*, 99, 191.
 Walker A. R., 1985, *MNRAS*, 213, 889.